Steady-State Electrochemical Determination of Lipidic Nanotube Diameter Utilizing An Artificial Cell Model

ARTICLE *in* ANALYTICAL CHEMISTRY · FEBRUARY 2010

Impact Factor: 5.64 · DOI: 10.1021/ac902282d · Source: PubMed

9 AUTHORS, INCLUDING:

Johan Engelbrektsson
SP Technical Research Institute of Sweden
10 PUBLICATIONS **149** CITATIONS

SEE PROFILE

Ann-Sofie Cans
Chalmers University of Technology
34 PUBLICATIONS **884** CITATIONS

SEE PROFILE

Andrew G Ewing
University of Gothenburg
191 PUBLICATIONS **5,324** CITATIONS

SEE PROFILE

Published in final edited form as:
Anal Chem. 2010 February 1; 82(3): 1020. doi:10.1021/ac902282d.

Steady-state electrochemical determination of lipidic nanotube diameter utilizing an artificial cell model

Kelly L. Adams[1,2], **Johan Engelbrektsson**[2], **Marina Voinova**[3], **Bo Zhang**[1,4], **Daniel J. Eves**[1], **Roger Karlsson**[2], **Michael L. Heien**[1], **Ann-Sofie Cans**[5], and **Andrew G. Ewing**[1,2,*]

[1] Department of Chemistry, 104 Chemistry Research Building, The Pennsylvania State University, University Park, PA USA 16802.

[2] Department of Chemistry, University of Gothenburg, SE-41296, Göteborg, Sweden

[3] Department of Physics, University of Gothenburg, SE-41296, Göteborg, Sweden

[4] Department of Chemistry, University of Washington, Seattle, WA, 98195

[5] Department of Chemical and Biological Engineering, Chalmers University of Technology, Göteborg, Sweden

Abstract

By exploiting the capabilities of steady-state electrochemical measurements, we have measured the inner diameter of a lipid nanotube using Fick's first law of diffusion in conjunction with an imposed linear concentration gradient of electroactive molecules over the length of the nanotube. Fick's law has been used in this way to provide a direct relationship between the nanotube diameter and the measurable experimental parameters Δi (change in current) and nanotube length. Catechol was used to determine the Δi attributed to its flux out of the nanotube. Comparing the nanotube diameter as a function of nanotube length revealed that membrane elastic energy was playing an important role in determining the size of the nanotube and was different when the tube was connected to either end of two vesicles or to a vesicle on one end and a pipette tip on the other. We assume that repulsive interaction between neck regions can be used to explain the trends observed. This theoretical approach based on elastic energy considerations provides a qualitative description consistent with experimental data.

INTRODUCTION

Membrane tethers have sparked great interest concerning their potential role in fundamental cellular operations as well as their function within biological mimics. Lipid tubes help facilitate both intra- and intercellular transport of surface proteins, vesicles, and other small membranous entities. More specifically, membranous tubes facilitate trafficking between organelles within the same cell, such as within the Golgi-ER complex[1, 2], but also between cells *in vitro*, for example, between specific cells contained in the immune system[3], or even different cell types entirely[4]. Aside from lipid nanotubes found in cells performing “active” shuttling of materials, artificial lipid nanotubes have been implemented as connective channels in miniaturized nanotube-vesicle networks analogous to microfluidic systems[5, 6]. These systems are constructed from soybean liposomes and have been used to study small-scale enzymatic reactions with mass transport-based mixing[7]. For a more comprehensive review of applications employing liposomes, the reader can consult Reference [8].

* Corresponding Author andrew.ewing@chem.gu.se fax: +46317722785.

Another variation of the nanotube-vesicle system has been developed into a suitable model to explore the role lipids play in the final stages of exocytosis, a process central to neuronal communication[9, 10]. The artificial cell model has a large, outer parent vesicle acting as a cell membrane and a small, inner vesicle connected by a lipid nanotube. This nanotube can be compared to the fusion pore created between the cell plasma membrane and the membrane of a synaptic vesicle. The synaptic vesicle diffuses to the plasma membrane surface, docks, and fuses, forming a fusion pore. Subsequently the pore dilates and the vesicle content is released into the extracellular space. If electroactive molecules are in the vesicle, their release can be detected electrochemically by a microelectrode positioned over the cell. We were highly motivated to further characterize this tube dimension within our model system. Knowledge of the tube diameter provides a better understanding of the physical nature of the membrane structure and thus lead to quantitative estimations of the magnitude and types of forces necessary to expel material through such an opening. For example, an osmotic pressure differential has been shown to increase the likelihood of “feet” in PC12 cells undergoing exocytosis[11]. These feet, manifested by small increases in current prior to the current transient associated with full release, represent small leakages of transmitter molecules from the vesicle through the initial fusion pore opening. This pre-release or a “foot” is detected electrochemically by the microelectrode positioned over the cell. Such leakage may be partially regulated by the physical dimensions of the pore opening thus making it an important parameter to measure.

Lipid nanotubes created from soy polar lipid extract have previously been estimated as having diameters in the 100- to 300-nanometer range. These estimates were based on two methods: a video pixel analysis[5] and a tube coalescence method[12] previously described by Cuvelier and coworkers[13]. Other methods such as transmission electron microscopy[14], freeze fracture electron microscopy[14, 15], scanning electron microscopy[16], atomic force microscopy[17], and lipid tether pulling experiments[18-20] have been employed to characterize membranous tubes. Most of these methods require a stable, non-fluidic sample in order to successfully carry out analysis. It is difficult to obtain a viable, fluidic sample to measure the tube dimensions in its dynamic, more biologically relevant state.

Electrochemical methods are ideally suited for measurements in aqueous environments. More specifically, steady-state amperometry is appropriate for measuring the net flux of electroactive material through a defined geometry. Previously steady-state electrochemistry was utilized to characterize a conical pore leading to a nanometer sized electrode[21], to evaluate the dimensions of a recessed nanometer-sized platinum nanoelectrode[22], and to characterize various nanostructures through impedance measurements[23].

In this paper, we utilize steady-state carbon fiber amperometry combined with a model of diffusion-based transport to determine the inner diameter of a lipid nanotube present in our liposome model of exocytosis. This nanotube mimics a fusion pore and more direct comparisons to this pore can be made with a well-characterized, known nanotube diameter. Additionally, two experimental configurations were examined where a lipid nanotube was either connected between two vesicles (two-vesicle configuration) or attached/adhered directly to a glass pipette on one end and the outer vesicle on the other (tube-only configuration). The results show significant differences in lipid nanotube diameter between the two different configurations when tube lengths were <10 μm. We report the direct measurement of the nanotube diameter versus nanotube length as calculated from steady-state current measurements. Finally, we present a theoretical model describing the differences between the two-vesicle and tube-only configurations.

EXPERIMENTAL SECTION

Chemicals and materials

The buffer for the liposome preparation was composed of 5 mM Trizma base/15 mM K_3PO_4/30 mM KH_2PO_4/10 mM K_2HPO_4/0.5 mM EDTA/1 mM $MgSO_4$ at pH 7.4. Dopamine, catechol, and chloroform were all used as received. All chemicals were of analytical grade and purchased from Sigma-Aldrich (Sweden). Borosilicate glass (1.0mm O.D., 0.78mm I.D.) was obtained from Harvard Apparatus, UK.

Liposome preparations and manipulations

Surface immobilized liposomes were made from soybean polar lipid extract (Avanti Polar Lipids, Alabaster, AL) using a dehydration/rehydration method described previously[10]. Briefly, 1 mg of soybean polar extract in chloroform was dried in a round-bottom flask using a rotation evaporator (Büchi, Switzerland). The dried lipid film was rehydrated with 1 mL of buffer and stored in the refrigerator for ~24 h. The flask was then sonicated for ~15 min prior to 5 μL of the lipid suspension being micropipetted onto a borosilicate coverslip (Menzel-Gläser, Braunschweig, Germany; 24mm × 60mm, #1) and subsequently dehydrated in a vacuum desiccator. The slide was transferred to the microscope and the film was rehydrated with buffer. This method yields liposomes of a specific lipid conformation: a unilamellar component attached to a multilamellar component that acts as a lipid reservoir.

Once this liposome conformation was identified, an injection pipette pulled with a commercial pipette puller (Model PE-21, Narishige Inc., London, UK) was back-filled with a 50 mM catechol solution and inserted into the unilamellar part of the liposome by means of a micromanipulator (Model MHW-3, Narishige, Inc, London, UK) with the aid of an electroporation voltage pulse (~30-50V, ~1 ms duration) generated by a constant voltage isolated stimulator (DS2A-Mk. II, Digitimer, Inc., Hertfordshire, UK). The counter electrode for electroporation was made from a pre-constructed 5-μm carbon fiber tip (ProCFE from Dagan Corp, Minneapolis, MN). This counter electrode was maneuvered opposite the injection pipette via another micromanipulator. The injection pipette was used to eject catechol solution (50 mM), by means of a Femtojet microinjector (Eppendorf / Brinkmann Instruments, Hauppauge, NY), into the unilamellar component.

Once the liposome was at a workable size (generally >50 μm in diameter), two different nanotube configurations were formed, examined, and compared. First, the injection pipette was manipulated to puncture through the second wall of the unilamellar liposome. The pipette was then slowly retracted into the interior of the parent vesicle, bringing with it lipid material adhered to the pipette tip and forming a lipid nanotube between parent vesicle and attachment pipette. This is the tube-only configuration and is illustrated in schematic A of Figure 1. Second, by injection of solution from the glass pipette, a small, inner vesicle (generally >5 μm in diameter) was created inside the parent vesicle with a lipid nanotube connection to the exterior. This is the two-vesicle configuration and is illustrated in schematic B of Figure 1. The inner vesicle for all experiments herein was filled with 50 mM catechol unless otherwise noted.

Microscopy and digital video recording

Liposome experiments were monitored using an Olympus IX-71 microscope (Olympus, Melville, NY) with a 40x oil objective (Olympus, UApo/340 40x oil iris, NA 1.35) using differential interference contrast (DIC) to give a pseudo-three dimensional appearance to the liposome. Experiments were visually recorded using an Olympus SC20 digital color camera interfaced to a personal computer with Cell-A software (Olympus, Hamburg, Germany). Nanotube lengths were measured within the Cell-A software from digital images captured during electrochemistry measurements.

Electrode fabrication and electrochemical data acquisition

Carbon fiber working electrodes were fabricated by aspirating isolated 5-μm diameter fibers into borosilicate glass capillaries (1.2 mm O.D., 0.69 mm I.D., Sutter Instrument Co., Novato, CA). The capillaries were subsequently pulled with a commercial micropipette puller (Model PE-21, Narishige, Inc., London, UK) and sealed with epoxy (Epoxy Technology, Billerica, MA). After beveling (Model BV-10, Sutter Instrument Co., Novato, CA) at 45 degrees and testing in 0.1 mM dopamine, electrodes were placed against the liposome-nanotube junction using a piezomicropositioner (PCS-750/1000, Burleigh Instruments, Fishers, NY). Working electrodes were held at +800 mV versus a silver/silver chloride reference electrode (Scanbur, Sweden) using an Axon 200B potentiostat (Molecular Devices, Sunnyvale, CA). The carbon fiber working electrode was placed against the parent liposome at the point of the nanotube exit. A Ag/AgCl reference electrode (Scanbur, Sweden) was placed in the solution surrounding the liposome preparation. The output from the potentiostat was digitized at 5 kHz and filtered at 2 kHz via an internal four-pole lowpass Bessel filter. The output was further filtered via a 10 Hz lowpass digital filter within the AxoScope 10.2 software (Molecular Devices, Sunnyvale, CA) prior to analysis via MiniAnalysis software (Synaptosoft, Inc., Decatur, GA)

Tube radius measurements

With the nanotube in place, the 5-μm carbon fiber electrode was placed at the nanotube-liposome junction and was allowed to rest until the current detected reached a stable, unchanging level. On average, this baseline was recorded for ~30 s. Once a stable baseline had been observed, the injection pipette was moved to either lengthen or shorten the nanotube length (L). After the new length was obtained, the measured current level was allowed to reestablish. This typically took as little as 10 s, but at times required several minutes. The reason for this is not entirely clear. This process of tube lengthening or shortening may be repeated several times for the same liposome. To obtain a background baseline measurement at the conclusion of an experiment, the electrode was maneuvered away from the nanotube-liposome junction and allowed to reach a steady-state current in the absence of electroactive species i.e. in buffer solution only. The difference in the measured current (Δi, illustrated by Figure 1) from this background can then be used to compute the diameter of the nanotube. Errors are reported as standard error of the mean.

RESULTS AND DISCUSSION

Initial nanotube measurements

Using a steady-state amperometric detection allows determination of both the nanotube diameter and the effect that tube length has on this calculated diameter. The approach uses a steady-state diffusion measurement assuming two conditions: (1) the concentration gradient for the electroactive species along the tube is linear, and (2) the effective concentration at the end of the nanotube (i.e. at the nanotube-liposome junction) is zero. The second condition results because the redox species is totally consumed at the electrode surface when using constant potential amperometry, maintaining the redox species concentration at zero at the outer nanotubeliposome junction. To quantify the results of our measurements, Fick's first law of diffusion was used, here written as diffusion through the nanotube as

$$J(\ell) = -D\frac{\partial C(\ell)}{\partial \ell} \tag{1}$$

where J is the flux of material at a given distance ℓ along the tube, D is the diffusion coefficient of the selected redox molecule (the bulk phase diffusion constant is used here assuming no substantial interactions with the double layer which has a Debye length a little less than 1 nm),

∂C is the change in concentration of the redox molecule at a given distance ℓ, and $\partial\ell$ is the change in distance along the tube. With the assumption that the concentration gradient along the tube length is constant, we can rewrite Equation 1 as follows:

$$\frac{\Delta i}{nFA} = D\left[\frac{dC}{d\ell}\right]_{\ell=0} \tag{2}$$

where Δi is the difference in current measured during the experiment, n is the number of moles of electrons transferred per mole of electroactive species, F is Faraday's constant (96,485 coulombs/mole electrons), and A is the cross-sectional area of the nanotube. Further substituting for the area of the tube cross-section, employing the assumption of a constant linear concentration gradient, and examining at a tube length (L) gives Equation 3 as

$$\frac{\Delta i}{nF\pi r^2} = D\frac{\Delta C}{L} \tag{3}$$

Solving for the radius gives

$$r = \sqrt{\frac{\Delta i}{nF\pi D\frac{\Delta C}{L}}} \tag{4}$$

This provides a relationship between the nanotube radius (or diameter when r is doubled) and the measurable experimental parameters Δi and L. For all experiments reported herein, catechol was the redox molecule used at a concentration of 50 mM, n is 2 moles of electrons per mole of catechol oxidized, and a diffusion coefficient (D) of 7.0×10^{-6} $cm^2 \cdot s^{-1}$ was used[24]. The neutral catechol was chosen again to limit interactions with a charged double layer in the nanotube. To determine the Δi attributed to catechol flux out of the nanotube, the steady-state current obtained without the nanotube present (background) was subtracted from the steady-state current established in the presence of the nanotube. A representative current versus time trace illustrating a typical Δi is shown in Figure 1.

A series of electrochemical measurements have been collected sequentially to generate a “staircase-like” current vs. time plot (Figure 2). Here a lipid nanotube has been pulled inside the parent vesicle to a starting length of ~17 μm. After a steady current was established (at t = ~20 s in Figure 2), the tube length was decreased to ~12 μm. This was accompanied by an increase in the measured current due to an anticipated increase in catechol flux through this new, shorter tube length. Decreasing the tube length further to ~7 μm brought about another current rise and a new, higher current level. This effect was reversible with the current levels subsequently decreasing upon increasing the nanotube length to ~13 μm and ~18 μm, respectively. The background current to be subtracted was determined at the conclusion of the experiment by maneuvering the electrode away from the nanotube-liposome junction (at t = ~120 s, Figure 2). Making measurements in this manner can help minimize small experimental variabilities due to electrode sensitivity and injection pipette tip sizes as well as interrogate a range of tube lengths for both configurations under nearly identical conditions.

Comparison of tube measurements in the two-liposome and tube-only configurations

Using the sequential method of data collection outlined above, the two-vesicle and tube-only configurations were investigated to examine the effect of liposome neck geometry on tube diameter. The two-vesicle mode is of particular interest with its relation to the fusion pore

between a cell and a releasing vesicle. The fusion pore is analogous to a small, hollow nanotube allowing materials to be exchanged from the vesicle interior to the extracellular space. Previously our laboratory has shown that the nanotube connecting the inner and parent vesicles in the liposome artificial cell model acts similarly to that observed for exocytotic release of dopamine from PC12 cells[10]. Likewise, the tube-only configuration is of interest for two reasons. First, this configuration could serve as a systematic control of the liposome-lipid nanotube model. Other studies suggest that tubes made by point-force methods using micropipettes have diameters independent of length[25]. Second, the tube-only configuration is similar to the structures used to obtain previous estimates of soybean lipid extract nanotube diameters. In particular, the aforementioned coalescence measurements required the lipidic tube to be directly adhered to the tip of the manipulation pipette.

Using the diffusion-based model (Equations 1-4) with its applied assumptions, a comparison of Δi relative to the inverse of tube length can be written as follows:

$$\Delta i = nF\pi r^2 D\Delta C\frac{1}{L} \tag{5}$$

Here the linear trend observed for Δi versus 1/L suggests the model is suitable for determining the nanotube dimensions over the range of nanotube lengths probed. This analysis assumes, however, that the diameter of the nanotube remains nearly constant over the range of nanotube lengths examined. As one can see from Figure 3, a linear trend for each configuration is observed. The apparent slopes differ, however, indicating different nanotube dimensions for the two configurations. An *average* tube diameter over the range of nanotube lengths investigated was calculated from the slope of the linear fit for Δi versus 1/L. The slope is the product of n, F, π, r^2, D, and ΔC as per Equation 5. The *average* tube diameter was found to be 114 ± 19 nm and 47 ± 7 nm for the tube-only and two-vesicle configurations, respectively. These values are close to the range estimated in the earlier work using a dynamic nanotube-liposome network as reported by Orwar and coworkers,[6] and in the range reported for systems using stable, non-fluidic samples.

Alternatively, the nanotube diameter can be directly computed via substitution of measured i and nanotube length into Equation 4. The resultant data for calculated nanotube diameter at a given length is shown in Figure 4. The two configurations yielded different relationships over the range of lengths examined. With a tube-only configuration (Figure 4, gray trace), a nearly constant tube diameter independent of nanotube length is suggested (123 ± 4 nm for 11 point measurements). Linear regression analysis confirmed the slope was statistically non-different from zero. The linear trend observed for the Δi vs. 1/L relationship (Figure 3) also supports this observation because this relationship assumes the nanotube dimension is independent of nanotube length. This agreement supports not only the validity of the measurement protocol, but also the electrochemical model with its basic assumptions.

Conversely, the two-vesicle configuration (Figure 4, black trace) exhibited a dependence on tube length. If the slope of the Δi vs. 1/L relationship is used to determine an *average* tube diameter for the two-vesicle configuration, the estimation will be considerably smaller than what is observed from individually calculated measurements. This is because, as revealed in Figure 4, the diameter is *not* independent of nanotube length.

Modeling the difference in the trend of diameter between nanotube configurations

The deviation of tube diameter with length at L<10 μm for the two-vesicle configuration might be attributed to the flexible, high curvature “neck” regions present (this is shown in the model in Figure 5). To investigate these differences, a simple model has been developed considering

that the two-vesicle system contains two flexible neck regions (one where the nanotube connects to the parent vesicle and one where the nanotube connects to the inner vesicle) and the tube-only configuration has just one flexible neck region (where the nanotube connects to the membrane of the parent vesicle). To model the effect of length on tube diameter, we assume that the neck region at the glass pipette-lipid interface is constant or "fixed" regardless of nanotube length[26]. This might be the dominant factor in determining lack of change in nanotube diameter as a function of length. Alternatively, one could use membrane properties to explain the data. Membrane properties that are dependent on tube length include membrane tension and bending rigidity. As this system contains a multilamellar reservoir of lipid, tension is essentially constant. However, as nanotube diameter is increased the bending energy is decreased driving the tube to wider diameter at longer tube lengths. We propose that the pipette-nanotube neck is constant and the energy of the remaining liposome-nanotube neck drives the tube to smaller diameter. The bending and neck energies counteract and lead to a nearly constant measured nanotube diameter as a function of length in the tube-only configuration.

The situation when two vesicles are present at either end of the nanotube is different. Experimentally, a larger tube dimension is observed at increased tube length. The thermodynamic bending energy of the tube is reduced as the tube diameter is larger. If the two flexible necks in this configuration energetically repel each other, this would result in a promotion of tube thinning at shorter tube lengths (Figure 5, arrows). The thinning brought about by neck repulsion could be in direct competition with the tube bending energy trying to expand its size, which would prevail at longer tube lengths. At shorter nanotube lengths (<10 μm), the interaction between the two necks must be taken into account in the free energy of the tube, thus driving the calculated tube diameter to be smaller than that observed for the tube-only configuration. As the distance between the two necks increases (i.e. by increasing nanotube length), the bending energy of the tube increases and appears to overcome and dominate the apparent reduced repulsive interaction between the necks.

The rigorous theoretical explanation for the neck interactions and their effect on tube diameter has been suggested. This model introduces a term for the changing energy of this neck interaction dependent on the distance that separates the necks. First the free energy of the membrane can be expressed as[27]

$$F=\int \frac{\kappa}{2}(2H)^2 dA+\sigma A - pV - fL \tag{6}$$

where κ is the bending rigidity, *H* is the mean curvature of the membrane, A is the surface area of the membrane, σ is the membrane surface tension, p is the interior pressure of the volume (V) enclosed by the membrane, and f is the point force necessary to pull the membrane a distance L. The elastic free energy of the overall system can be expressed as a sum of the individual contributions of the membrane geometries present

$$F_{TOTAL}=F_V+F_T+F_N+F_{INTER} \tag{7}$$

where F_{TOTAL} is the total elastic energy of the system equaling the sum of the elastic energy of the vesicles (F_V), the nanotube (F_T), the neck regions (F_N), and the neck interaction (F_{INTER}). For our experimental set-up, we can assume F_V, F_T, and F_N are constant and independent of tube length[25], thus we can combine F_{INTER} with the bending energy to derive how these two energies can influence the tube diameter as length is varied. F_{INTER} for the two-vesicle and tube-only configurations can be expressed as

$$F_{INTER(Two-Vesicles)} = \frac{R_t^2}{L^\alpha} \quad (8)$$

$$F_{INTER(Tube-Only)} = \frac{R_t R_2}{L^\alpha} \quad (9)$$

where R_t is nanotube radius, R_2 is the radius of the tube closest to the orifice of the injection pipette, and L is the distance separating the necks (which is analogous to the nanotube length) with model fitting parameter α. R_2 was assumed to be constant relative to tube length according to Bensimon and coworkers[26]. Using the formula for the free elastic energy expression for the membrane, we phenomenologically observe α to be ⅓ and 1 for two-vesicle and tube-only, respectively. This is consistent with the theory that at short nanotube lengths the neck interactions have a greater effect on the nanotube diameter and at long nanotube lengths the lipid bending energy effects are more likely to dominate.

CONCLUSIONS

By exploiting the capabilities of steady-state electrochemical measurements, we have measured the inner diameter of a lipid nanotube using Fick's first law of diffusion in conjunction with an imposed linear concentration gradient of electroactive molecules over the length of the nanotube. Comparing the nanotube diameter to the corresponding nanotube length suggested membrane elastic energy was important in determining the size of the tube and differed when the nanotube was connected on either end to two vesicles or to a vesicle on one end and a pipette tip on the other. We assumed that a repulsive interaction between neck regions could be used, in part, to explain the trends observed. A more rigorous approach based on the minimization of the elastic energies of the different regions of the nanotube, vesicles, and connecting necks was consistent with this assumption. As a final comment, these data also exemplify that electrochemical measurements can be used in special cases to exceed the limits of dimensional analysis for optical microscopy.

Acknowledgments

This work was supported by funding from the National Institutes of Health (A.G.E.) and the Swedish Research Council (A.G.E. and A.S.C). A.G.E. is supported by a Marie Curie Chair from the European Union 6th Framework. A.S.C. acknowledges research support the Knut and Alice Wallenberg Foundation.

REFERENCES

1. Hirschberg K, Miller CM, Ellenberg J, Presley JF, Siggia ED, Phair RD, Lippincott-Schwartz J. J Cell Biol 1998;143:1485–1503. [PubMed: 9852146]
2. Polishchuk RS, Polishchuk EV, Marra P, Alberti S, Buccione R, Luini A, Mironov AA. J Cell Biol 2000;148:45–58. [PubMed: 10629217]
3. Onfelt B, Nedvetzki S, Yanagi K, Davis DM. J Immunol 2004;173:1511–1513. [PubMed: 15265877]
4. Rustom A, Saffrich R, Markovic I, Walther P, Gerdes HH. Science 2004;303:1007–1010. [PubMed: 14963329]
5. Karlsson M, Sott K, Cans AS, Karlsson A, Karlsson R, Orwar O. Langmuir 2001;17:6754–6758.
6. Karlsson R, Karlsson M, Karlsson A, Cans AS, Bergenholtz J, Akerman B, Ewing AG, Voinova M, Orwar O. Langmuir 2002;18:4186–4190.
7. Karlsson A, Sott K, Markstrom M, Davidson M, Konkoli Z, Orwar O. Journal of Physical Chemistry B 2005;109:1609–1617.

8. Jesorka A, Orwar O. Annual Review of Analytical Chemistry 2008;1:801–832.
9. Cans AS, Wittenberg N, Eves D, Karlsson R, Karlsson A, Orwar O, Ewing A. Analytical Chemistry 2003;75:4168–4175. [PubMed: 14632131]
10. Cans AS, Wittenberg N, Karlsson R, Sombers L, Karlsson M, Orwar O, Ewing A. Proc Natl Acad Sci U S A 2003;100:400–404. [PubMed: 12514323]
11. Sombers LA, Wittenberg NJ, Maxson MM, Adams KL, Ewing AG. ChemPhysChem 2007;8:2471–2477. [PubMed: 17966970]
12. Tokarz M, Hakonen B, Dommersnes P, Orwar O, Akerman B. Langmuir 2007;23:7652–7658. [PubMed: 17547424]
13. Cuvelier D, Derenyi I, Bassereau P, Nassoy P. Biophysical Journal 2005;88:2714–2726. [PubMed: 15695629]
14. Polidori A, Michel N, Fabiano AS, Pucci B. Chem Phys Lipids 2005;136:23–46. [PubMed: 15921670]
15. Lauf U, Fahr A, Westesen K, Ulrich AS. ChemPhysChem 2004;5:1246–1249. [PubMed: 15446752]
16. Brazhnik KP, Vreeland WN, Hutchison JB, Kishore R, Wells J, Helmerson K, Locascio LE. Langmuir 2005;21:10814–10817. [PubMed: 16262357]
17. Kameta N, Masuda M, Minamikawa H, Shimizu T. Langmuir 2007;23:4634–4641. [PubMed: 17355159]
18. Bo L, Waugh RE. Biophysical Journal 1989;55:509–517. [PubMed: 2930831]
19. Hochmuth RM, Wiles HC, Evans EA, Mccown JT. Biophysical Journal 1982;39:83–89. [PubMed: 7104454]
20. Waugh RE, Hochmuth RM. Biophysical Journal 1987;52:391–400. [PubMed: 3651558]
21. Zhang B, Zhang Y, White HS. Analytical Chemistry 2006;78:477–483. [PubMed: 16408930]
22. Sun P, Mirkin MV. Journal of the American Chemical Society 2008;130:8241–8250. [PubMed: 18540603]
23. Sun L, Crooks RM. Journal of the American Chemical Society 2000;122:12340–12345.
24. Durgbanshi A, Kok WT. Journal of Chromatography A 1998;798:289–296.
25. Frolov VA, Lizunov VA, Dunina-Barkovskaya AY, Samsonov AV, Zimmerberg J. Proc Natl Acad Sci U S A 2003;100:8698–8703. [PubMed: 12857952]
26. Michalet X, Bensimon D, Fourcade B. Phys Rev Lett 1994;72:168–171. [PubMed: 10055593]
27. Derenyi I, Julicher F, Prost J. Phys Rev Lett 2002;88:238101. [PubMed: 12059401]

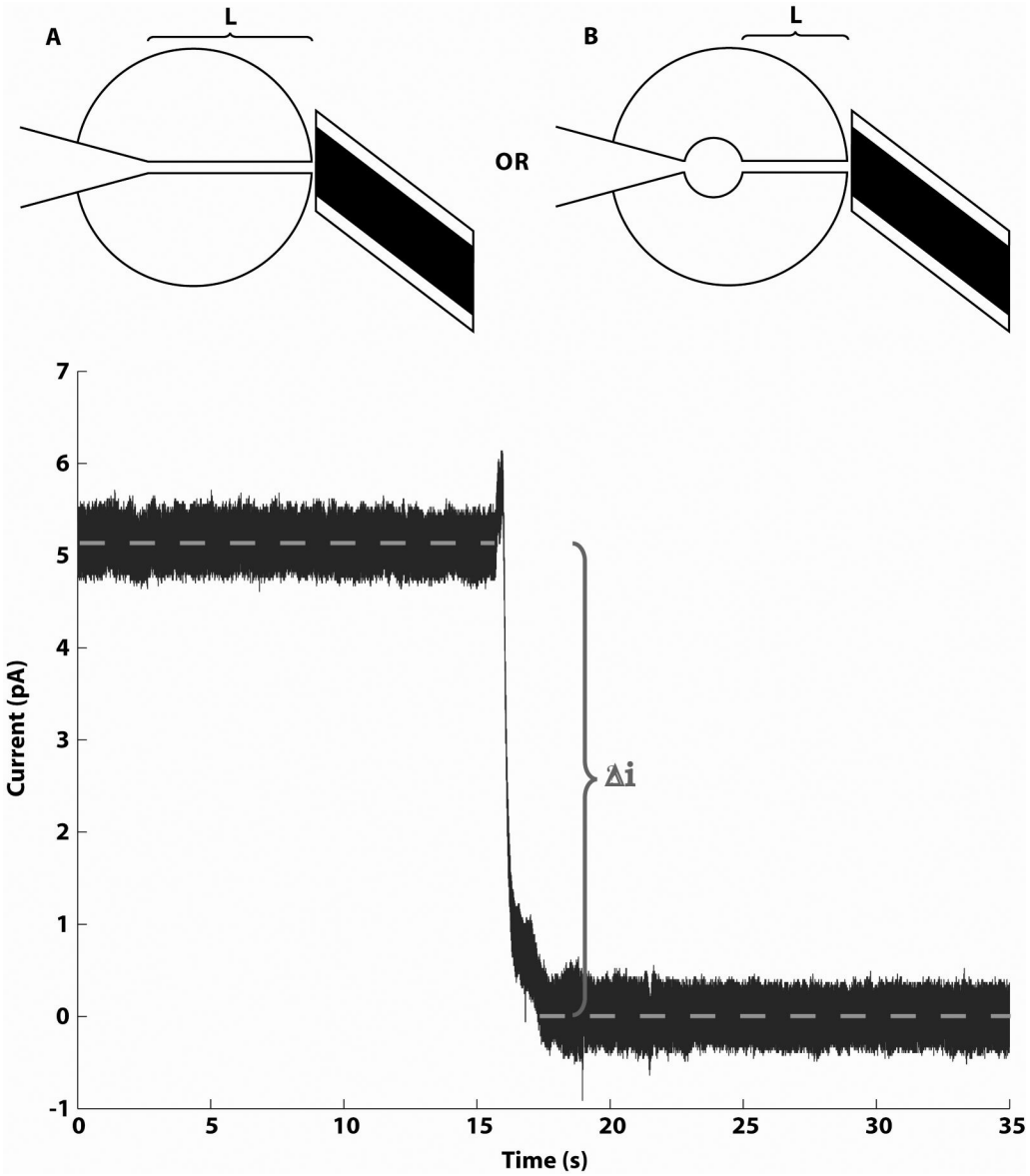

Figure 1.

Representative current vs. time amperometric trace (bottom) illustrating how the change in current (Δi) was measured. A steady-state current due to flux of material through the nanotube was measured in the tube-only configuration for this example. The background steady-state current was then established by removing the electrode from the nanotube-liposome junction, indicated by the ~5 pA drop in baseline current. This corresponded to a calculated tube diameter of ~127 nm for a tube ~17 μm in length. Schematics A and B represent the tube-only and two-vesicle configurations, respectively, and L indicates the nanotube length.

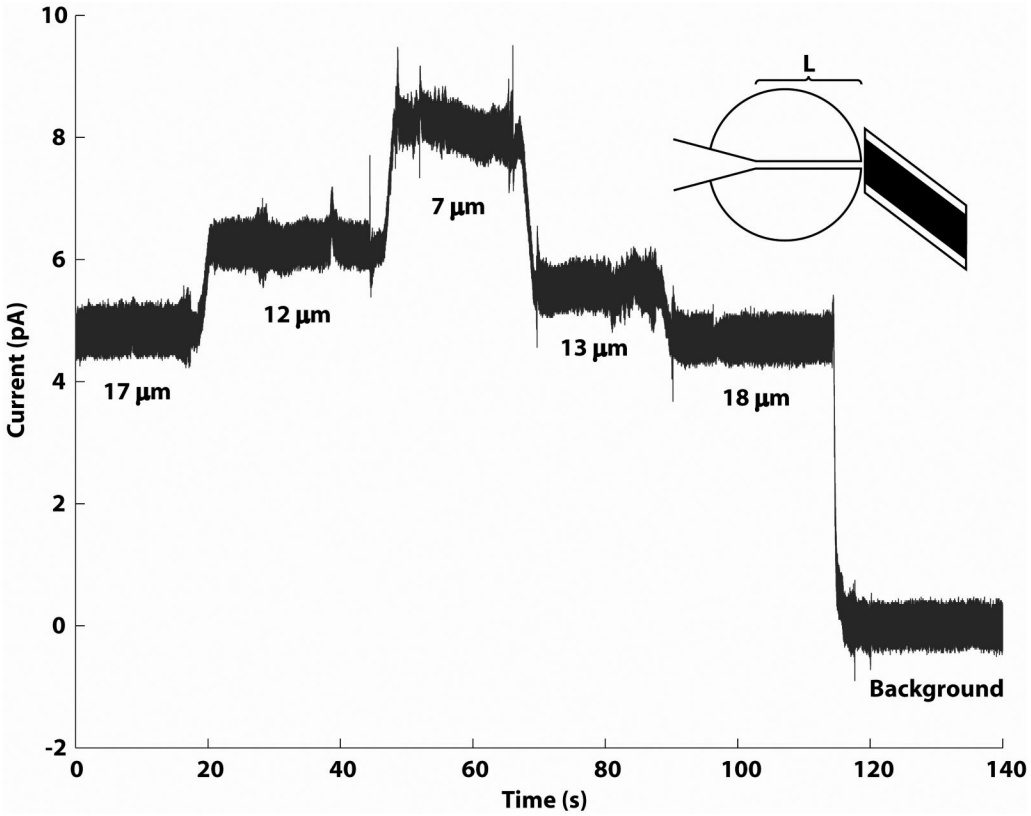

Figure 2.

Representative current vs. time amperometric trace for a tube-only configuration experiment. The steady-state currents for a series of 5 nanotube lengths (indicated below each baseline) from the same liposome generate a staircase-like amperometric trace when collected sequentially. At the end of the series, the background steady-state current was established by removing the electrode from the nanotube-liposome junction.

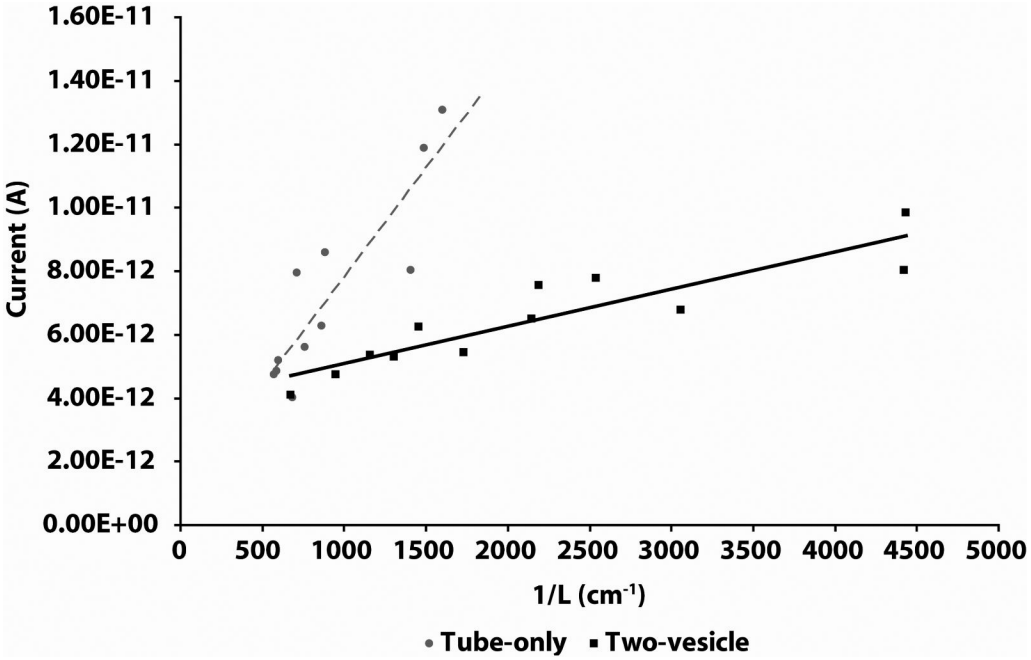

Figure 3.

Measured current versus inverse of the nanotube length for two-vesicles (■) and tube-only configuration (●). The linear fits verify that the diffusion-based model and applied assumptions can be used to approximate the *average* diameter of the nanotube.

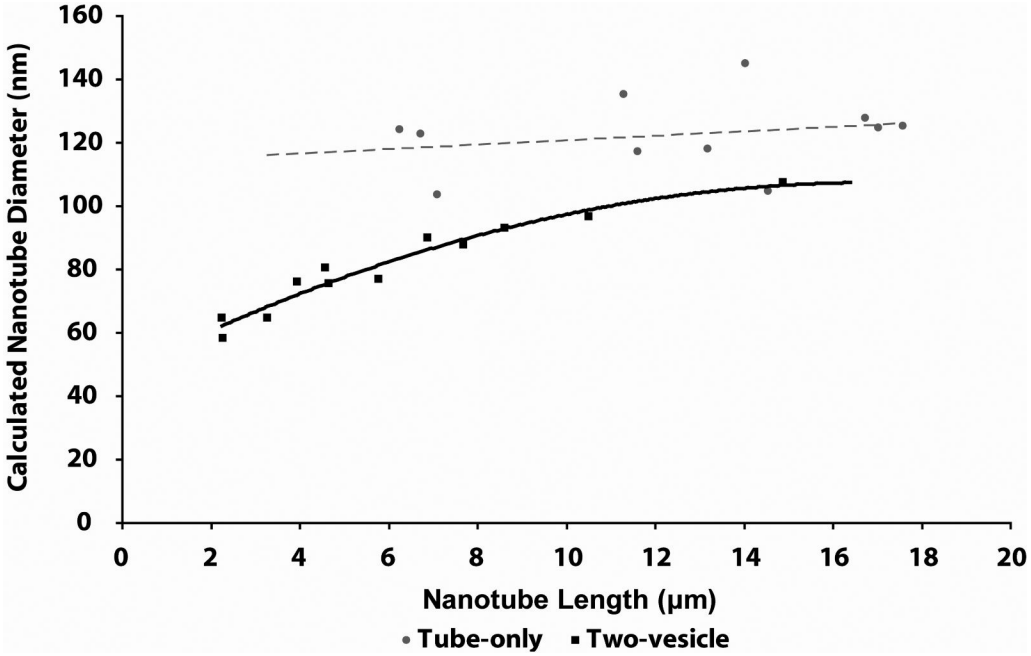

Figure 4.

Calculated diameter versus nanotube length for the two-vesicle configuration (■) and the tube-only configuration (●); n=3 different liposome preparations were used to obtain the data points for each configuration. Single data points are shown with 2 to 4 obtained from each preparation. Total number of data points (n) for each preparation is 11 and 12. Lines represent quadratic and linear fits for two-vesicle and tube-only, respectively.

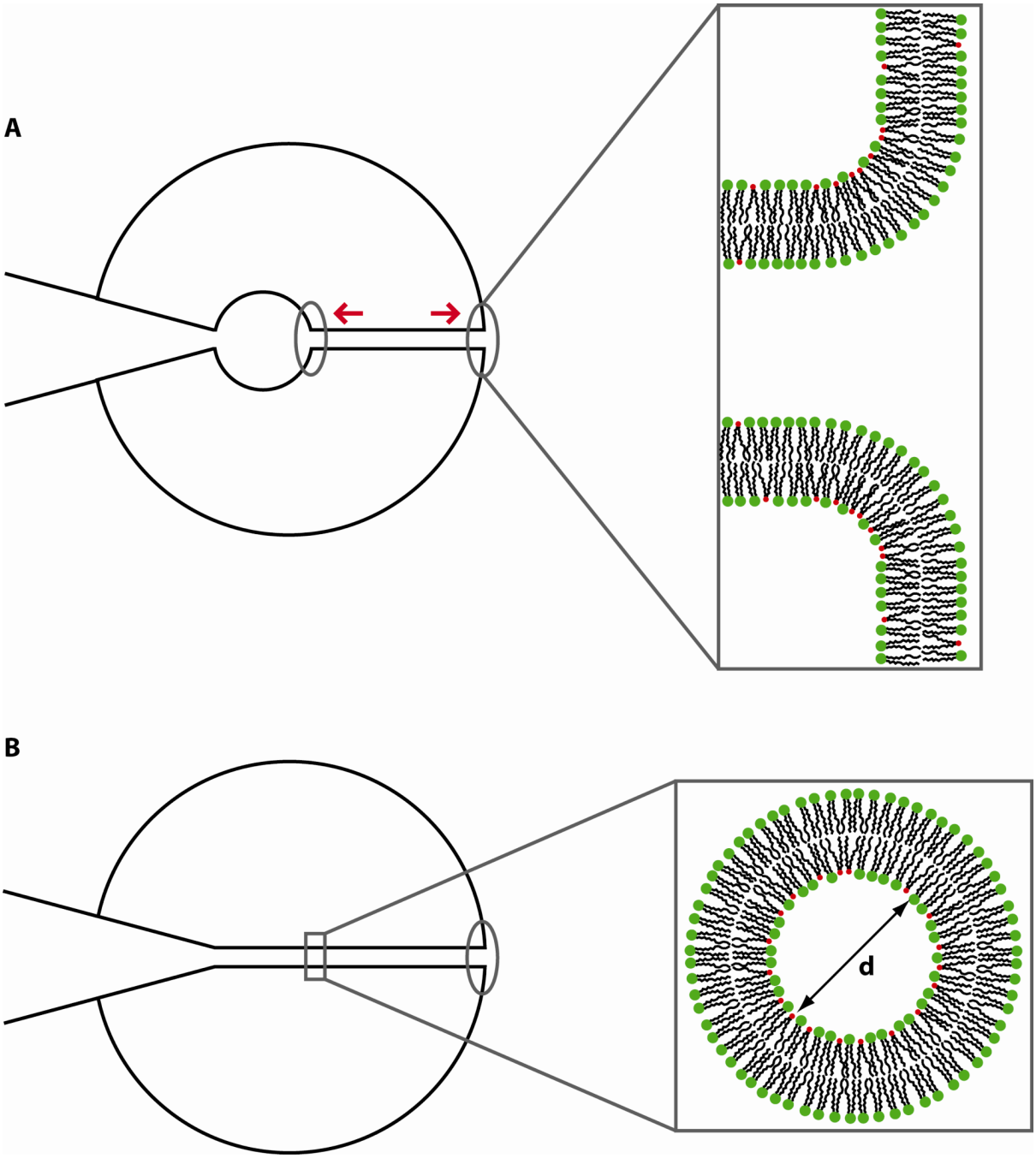

Figure 5.
Model of the two-vesicle (A) and tube-only (B) configurations. The grey ovals indicate where the flexible neck regions are located in each configuration. The red arrows represent the repulsion of the necks present in the 2 vesicle configuration. The enlargement in A is a side-view of the flexible neck region present in both configurations. Here the nanotube continues into the outer parent vesicle membrane via a junction of high curvature. The enlargement in B is a cross-sectional view of the nanotube present in both configurations with the inner diameter (d) indicated. The lipids are not drawn to scale.